

Hybrid Nanorod-Polymer Solar Cells

Wendy U. Huynh, Janke J. Dittmer, A. Paul Alivisatos*

We demonstrate that semiconductor nanorods can be used to fabricate readily processed and efficient hybrid solar cells together with polymers. By controlling nanorod length, we can change the distance on which electrons are transported directly through the thin film device. Tuning the band gap by altering the nanorod radius enabled us to optimize the overlap between the absorption spectrum of the cell and the solar emission spectrum. A photovoltaic device consisting of 7-nanometer by 60-nanometer CdSe nanorods and the conjugated polymer poly-3(hexylthiophene) was assembled from solution with an external quantum efficiency of over 54% and a monochromatic power conversion efficiency of 6.9% under 0.1 milliwatt per square centimeter illumination at 515 nanometers. Under Air Mass (A.M.) 1.5 Global solar conditions, we obtained a power conversion efficiency of 1.7%.

The widespread expansion in the use of inorganic solar cells remains limited due to the high costs imposed by fabrication procedures involving elevated temperature (400° to 1400°C), high vacuum, and numerous lithographic steps. Organic solar cells that use polymers which can be processed from solution have been investigated as a low-cost alternative with solar power efficiencies of up

Department of Chemistry, University of California, Berkeley and Materials Science Division, Lawrence Berkeley National Laboratory, Berkeley, CA 94720, USA.

*To whom correspondence should be addressed. E-mail: alivis@uclink4.berkeley.edu

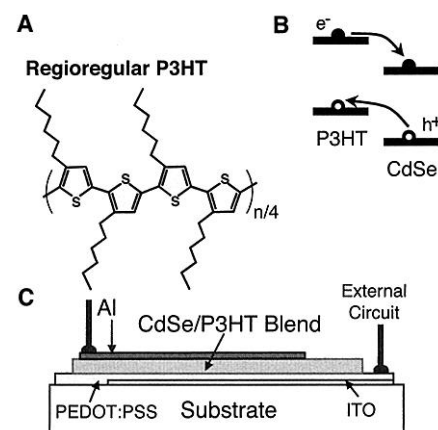


Fig. 1. (A) The structure of regioregular P3HT. (B) The schematic energy level diagram for CdSe nanorods and P3HT showing the charge transfer of electrons to CdSe and holes to P3HT. (C) The device structure consists of a film ~200 nm in thickness sandwiched between an aluminum electrode and a transparent conducting electrode of PEDOT:PSS (Bayer AG, Pittsburgh, PA), which was deposited on an indium tin oxide glass substrate. The active area of the device is 1.5 mm by 2.0 mm. This film was spin-cast from a solution of 90% wt % CdSe nanorods in P3HT in a pyridine-chloroform solvent mixture.

to 2.5% (1). Nonetheless, conventional inorganic solar cells routinely exhibit solar power conversion efficiencies of 10%, and the most advanced, but also the most expensive models, can reach up to 30% efficiency (2). The main factor for the superior efficiency of inorganic over organic devices lies in the high intrinsic carrier mobilities that exist in inorganic semiconductors. Higher carrier mobilities mean that charges are transported to the electrodes more quickly, which reduces current losses via recombination. For many conjugated polymers, electron mobilities are extremely low, typically below 10^{-4} $\text{cm}^2\text{V}^{-1}\text{s}^{-1}$, due to the presence of ubiquitous electron traps such as oxygen (3). Therefore, polymer photovoltaic (PV) devices rely on the introduction of another material for electron transport. The presence of a second material also provides an interface for charge transfer. Compounds such as small conjugated molecules, therefore, have been blended with polymers at a concentration that enables the formation of percolation pathways for electron transport (1, 4–6). The efficiency of these devices is limited by inefficient hopping charge transport (7), and electron transport is further hindered by the presence of structural traps in the form of incomplete pathways in the percolation network (6).

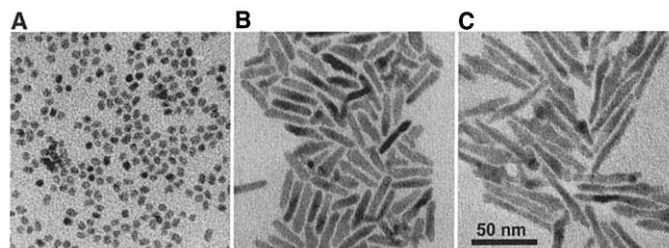
One way to overcome these charge transport limitations is to combine polymers with inor-

ganic semiconductors. Charge transfer is favored between high electron affinity inorganic semiconductors and relatively low ionization potential organic molecules and polymers (8, 9). Charge transfer rates can be remarkably fast in the case of organics that are chemically bound to nanocrystalline and bulk inorganic semiconductors, which have a high density of electronic states (10). Because of the nanoscale nature of light absorption and photocurrent generation in solar energy conversion, the advent of methods for controlling inorganic materials on the nanometer scale opens new opportunities for the development of future generation solar cells. Therefore, we have used colloidal semiconducting nanorods as the inorganic phase in the construction of these solar cells via solution-phase nano-assembly. By varying the radius of the rods, the quantum size effect can be used to control the band gap; furthermore, quantum confinement leads to an enhancement of the absorption coefficient compared with the bulk, such that devices can be made thinner (11). One-dimensional (1D) nanorods are preferable to quantum dots or sintered nanocrystals in solar energy conversion, because they naturally provide a directed path for electrical transport. The length of the nanorods can be adjusted to the device thickness required for optimal absorption of incident light.

We have established recently that both diameter and length of colloidal semiconductor nanorods of CdSe can be systematically varied to aspect ratios above 20 and lengths greater than 100 nm using a solution phase synthesis at temperatures below 300°C (12, 13). Here, CdSe nanorods were combined with the conjugated polymer poly(3-hexylthiophene) (P3HT) (Fig. 1A) to create charge transfer junctions with high interfacial area. From the schematic energy level diagram for CdSe nanocrystals and P3HT, it can be seen that CdSe is electron-accepting and P3HT is hole-accepting (Fig. 1B). CdSe is used as the electron transport material, whereas P3HT is an effective hole transport material in its regioregular form, demonstrating the highest field effect hole mobilities observed in polymers so far [reaching up to $0.1 \text{ cm}^2\text{V}^{-1}\text{s}^{-1}$ (14)].

The mechanical properties of P3HT allow for the room-temperature solution-casting of uniform, flexible thin films. However, dispersing the inorganic nanorods at high density with-

Fig. 2. Cadmium selenide nanocrystals with aspect ratios ranging from 1 to 10. The samples, shown by transmission electron micrographs (TEMs) at the same scale, have dimensions (A) 7 nm by 7 nm, (B) 7 nm by 30 nm, and (C) 7 nm by 60 nm.



in P3HT to facilitate charge transfer is a challenge because the complex surface chemistry of the nanocrystals can limit its solubility in the polymer. In Fig. 2, nanocrystals of 7 nm diameter and various lengths of up to 60 nm are shown. As nanocrystals increase in aspect ratio from spherical to rod-like, they move from the

molecular regime closer to the realm of a 1D wire and they become less readily soluble. Although we can control microphase separation and aggregation for low-aspect ratio CdSe nanocrystals dispersed in polymers (Fig. 3A), the performance of the resulting PV device is limited by inefficient hopping electron transport

(15). In order to accommodate high-aspect ratio nanorods, we developed a solvent mixture consisting of a good solvent and ligand for CdSe nanorods and a good solvent for the polymer. Nanorods were co-dissolved with P3HT in a mixture of pyridine and chloroform and spin-cast to create a uniform film consisting of dispersed nanorods in polymer (Fig. 3B) (16). We show that by controlling the aspect ratio of CdSe nanorods dispersed in P3HT, we can tailor the length scale and direction of electron transport through a thin film PV device.

We fabricated an efficient inorganic-organic hybrid solar cell by spin-casting a solution of 90% by weight (90 wt %) CdSe nanorods in P3HT onto an indium tin oxide glass substrate coated with poly(ethylene dioxythiophene) doped with polystyrene sulfonic acid (PEDOT:PSS, a conducting polymer) with aluminum as the top contact (Fig. 1C). With CdSe nanorods 7 nm by 60 nm, a power conversion efficiency of 6.9% was obtained under 0.1 mW/cm² illumination at 515 nm inside an inert atmosphere of flowing argon. For plastic PV devices, this monochromatic power conversion efficiency is one of the highest reported (1). At this intensity, the open-circuit voltage is 0.5 V, the photovoltage at the maximum power point is 0.4 V, and the fill factor (FF) is 0.6 (Fig. 4B). When our devices were tested in simulated sunlight [under A.M. 1.5 Global solar conditions and flowing argon (18)], a power conversion efficiency of 1.7%, an open-circuit voltage of 0.7 V, a photovoltage at maximum power point of 0.45 V, and a FF of 0.4 were obtained (Fig. 4C) (17). The maximum open-circuit voltage is determined by the difference between the work functions of the electrodes, PEDOT:PSS, and aluminum, as well as the difference between the lowest unoccupied energy level in the CdSe nanorod and the highest occupied energy level in P3HT. This difference is close to what we obtained at solar intensity.

Because CdSe and P3HT have complementary absorption spectra in the visible spectrum, these nanorod-polymer blend devices have a very broad photocurrent spectrum extending from 300 to 720 nm (Fig. 4A). Unlike other electron acceptors such as C₆₀ in organic blend devices and sintered TiO₂ in dye-sensitized solar cells, CdSe nanorods absorb a large part of the solar spectrum (1, 19). Furthermore, the absorption spectrum of the hybrid devices presented here can be tuned by altering the diameter of the nanorods in order to optimize the overlap with the solar emission spectrum (Fig. 4D). The onset of absorption for 60-nm-long nanorods with 3 nm diameter is at a wavelength of 650 nm, whereas the onset for those with 7 nm diameter is at 720 nm. Because P3HT shows no absorption beyond 650 nm, we can tune the onset of the photocurrent action spectrum from 650 to 720 nm by increasing the diameter of the nanorods while maintaining a constant length. The characteristics of these two devices, such as

Fig. 3. Thin films of 20 wt % (A) 7 nm by 7 nm and (B) 7 nm by 60 nm CdSe nanocrystals in P3HT were studied via transmission electron microscopy. In (C), a TEM of a cross section of a film with 60 wt % 10 nm by 10 nm CdSe nanocrystals in P3HT reveals the distribution and organization of nanoparticles across the 110-nm-thick film. A solution of CdSe in P3HT was spin-cast onto a Polybed epoxy substrate (Ted Pella, Redding, CA) and we used an ultramicrotome to obtain ultrathin cross sections. In (D), a TEM of a cross section of a 100-nm-thick film consisting of 40 wt % 7 nm by 60 nm CdSe nanorods in P3HT reveals that most nanorods are partially aligned perpendicular to the substrate plane. The solutions were cast onto an Epon/Aradite epoxy substrate (Ted Pella), embedded into epoxy, cured, and sliced using an ultramicrotome. This extra support is required to slice the nanorods with the microtome, because the blend film has a tendency to tear as the rods get longer.

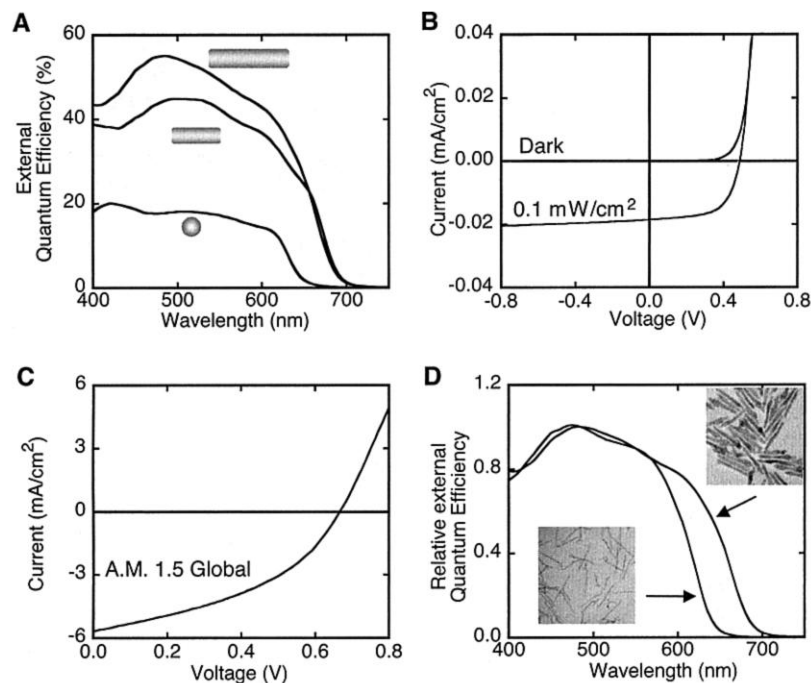
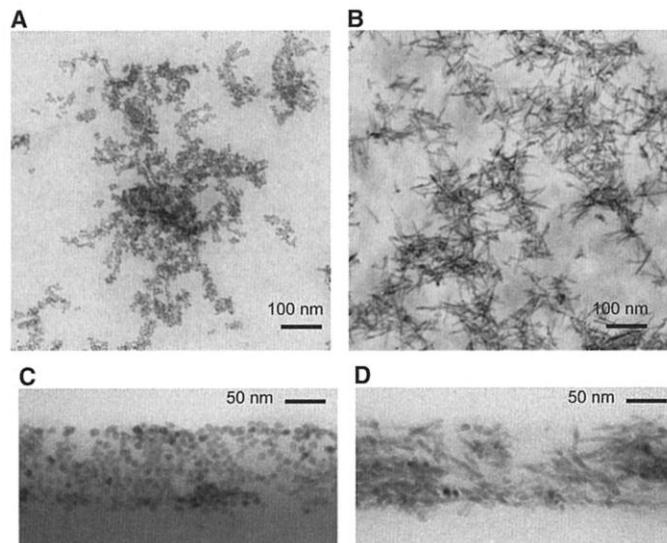


Fig. 4. (A) EQEs of 7-nm-diameter nanorods with lengths 7, 30, and 60 nm. The intensity is at 0.084 mW/cm² at 515 nm. (B) The current-voltage characteristics of the 7 nm by 60 nm nanorod device exhibit rectification ratios of 10⁵ in the dark and a short-circuit current of 0.019 mA/cm² under illumination of 0.084 mW/cm² and at 515 nm. (C) Solar cell characteristics of this 7 nm by 60 nm nanorod device illuminated with simulated AM 1.5 Global light, include a short-circuit current of 5.7 mA/cm². (D) Photocurrent spectra for two devices with 60-nm-long nanorods with diameters 7 and 3 nm.

open-circuit voltage and fill factor, are comparable. This further suggests that nanorod length not diameter determines device performance. Moreover, band gap tuning in nanorods enables the realization of high-efficiency device architectures, such as tandem solar cells in which the different band gaps can be obtained by modifying only one chemical compound.

We can understand the origin of the high efficiency of nanorod-polymer devices by studying the dependence of charge transport on nanorod length. The external quantum efficiency (EQE), which is the percentage of electrons collected per incident photon (with no correction for reflection losses), can be used as a measure of the efficiency of charge transport given that the following quantities are comparable for a set of devices: (i) incident light intensity; (ii) fraction of light absorbed; (iii) charge collection efficiency at the electrodes, which is mainly given by the choice of electrodes; and (iv) the charge transfer efficiency, as determined from photoluminescence quenching. These four conditions are met for the devices for which EQE data are presented in Fig. 4A. Therefore, we can conclude that as the aspect ratio of the nanorods increases from 1 to 10, the charge transport must improve substantially to yield an EQE enhancement by a factor of approximately 3. In networks consisting of shorter nanoparticles, electron transport is dominated by hopping and, in those consisting of longer particles, band conduction is prevalent. In a cross section of the blend film (Fig. 3D), most nanorods were oriented partly in the direction of the electric field and, thus, in the direction of electron transport. Because the thickness of the nanorod-polymer film is ~ 200 nm, 60-nm-long nanorods can penetrate through a large portion of the device whereas 30-nm and 7-nm-long particles are progressively less effective (Fig. 3C). The best device, which contained 7 nm by 60 nm nanorods, performed with a maximum EQE of 55% under 0.1 mW/cm² illumination at 485 nm (Fig. 4A), and this value has been remarkably reproducible (20).

In order for plastic nanorod devices to achieve typical power conversion efficiencies of conventional inorganic solar cells, it is necessary to reduce charge recombination, which decreases the EQE and the FF at solar light intensities. An increase in carrier mobilities would realize this by decreasing the carrier concentration within the device. Further enhancement of carrier mobilities can be accomplished by improving the nanocrystal-polymer interface to remove nanorod surface traps, aligning the nanorods perpendicular to the substrate, and further increasing their length.

References and Notes

1. S. E. Shaheen *et al.*, *Appl. Phys. Lett.* **78**, 841 (2001).
 2. M. A. Green, K. Emery, D. L. King, S. Igarai, W. Warta, *Prog. Photovoltaics* **9**, 287 (2001).

3. L. Bozano, S. A. Carter, J. C. Scott, G. G. Malliaras, P. J. Brock, *Appl. Phys. Lett.* **74**, 1132 (1999).
 4. G. Yu, J. Gao, J. C. Hummelen, F. Wudl, A. J. Heeger, *Science* **270**, 1789 (1995).
 5. L. S. Roman, M. R. Andersson, T. Yohannes, O. Inganäs, *Adv. Mater.* **9**, 1164 (1997).
 6. J. J. Dittmer, E. A. Marsiglia, R. H. Friend, *Adv. Mater.* **12**, 1270 (2000).
 7. H. Bässler, *Molec. Cryst. Liq. Cryst. Sci. Technol. Sec. A* **252**, 11 (1994).
 8. N. C. Greenham, X. G. Peng, A. P. Alivisatos, *Phys. Rev. B* **54**, 17628 (1996).
 9. D. S. Ginger, N. C. Greenham, *Phys. Rev. B* **59**, 10622 (1999).
 10. J. M. Rehm *et al.*, *J. Phys. Chem.* **100**, 9577 (1996).
 11. A. P. Alivisatos, *Science* **271**, 933 (1996).
 12. X. G. Peng *et al.*, *Nature* **404**, 59 (2000).
 13. Z. A. Peng, X. G. Peng, *J. Am. Chem. Soc.* **123**, 183 (2001).
 14. H. Sirringhaus, N. Tessler, R. H. Friend, *Science* **280**, 1741 (1998).
 15. W. U. Huynh, X. G. Peng, A. P. Alivisatos, *Adv. Mater.* **11**, 923 (1999).
 16. We used between 5 and 15% pyridine in chloroform. The optimal amount of pyridine is determined by the number of nonpassivated Cd surface sites on the nanorods. An excess of pyridine, however, is to be avoided, as this mediates the precipitation of P3HT, which is insoluble in pyridine. Replacing chloroform with this solvent mixture leads to an increase in energy conversion efficiency of more than 50%.
 17. The FF is defined as $FF = \frac{(I \cdot V)_{\max}}{I_{sc} \cdot V_{oc}}$ where I_{sc} and V_{oc} are short circuit current and open circuit voltage, respectively. The power conversion efficiency is $\eta = \frac{FF \cdot I_{sc} \cdot V_{oc}}{\text{light intensity}}$. The power conversion efficiency can be calculated both under monochromatic and white light (such as solar) illumination.
 18. The sun simulator essentially consists of a 75 W xenon source and a set of Oriol A.M. 0 and A.M. 1.5 filters (Stratford, CT). The temperature was maintained at 25°C, verified by an in situ thermocouple by flowing argon past the device during measurements. The spectral overlap and intensity integral between the A.M. 1.5 Global standard (with spectral standard, ASTM E892 Global, and intensity of 96.4 mW/cm²) and our sun simulator were optimized for the wavelength region in which the active layer shows absorption. The error in the simulation with regards to the obtained photocurrent is $\sim 10\%$.
 19. B. O'Regan, M. Grätzel, *Nature* **353**, 737 (1991).
 20. The results reported represent the median of five sets of devices made on separate occasions from three different synthetic batches of CdSe totaling 57 individual solar cells. The maximum external quantum efficiency of each of these 57 devices are all within 10% relative to the median with the highest obtained efficiency at 59%, all under ~ 0.1 mW/cm² monochromatic illumination. Individual devices have been characterized repeatedly over the time scale of several months and showed no substantial change between measurements.
 21. Supported by the National Renewable Energy Laboratory (grant XAD-9-18668-02) and the DOE (contracts DE-AC03-76SF00098 and DE-AC03-76SF00098). We are grateful to the Robert D. Ogg Electron Microscopy Laboratory at the University of California, Berkeley, for assistance with the TEM work and providing cross sections. The authors also would like to thank G. Whiting and W. Libby for experimental assistance and L. Manna, D. Milliron, J. Frechet, and C. Pitois for their valuable discussions. W.U.H. thanks the Natural Sciences and Engineering Research Council of Canada for a fellowship.

19 December 2001; accepted 19 February 2002

Theory of Quantum Annealing of an Ising Spin Glass

Giuseppe E. Santoro,¹ Roman Martoňák,^{2,3} Erio Tosatti,^{1,4*} Roberto Car⁵

Probing the lowest energy configuration of a complex system by quantum annealing was recently found to be more effective than its classical, thermal counterpart. By comparing classical and quantum Monte Carlo annealing protocols on the two-dimensional random Ising model (a prototype spin glass), we confirm the superiority of quantum annealing relative to classical annealing. We also propose a theory of quantum annealing based on a cascade of Landau-Zener tunneling events. For both classical and quantum annealing, the residual energy after annealing is inversely proportional to a power of the logarithm of the annealing time, but the quantum case has a larger power that makes it faster.

The annealing of disordered and complex systems toward their optimal (or lowest energy) state is a central problem in statistical physics. The unknown ground state of a system can be approximated by slow-rate cooling of a real or fictitious temperature: The slower the cooling, the closer the approximation gets to the optimal solution (1, 2). Although this kind of standard classical annealing (CA) has been extensively investigated over the last two decades (1–3) and is routinely used in a variety of technological applications, such as chip circuitry

design, any improved optimization algorithm would certainly be of enormous value.

Recent results on the spin $\frac{1}{2}$ disordered Ising ferromagnet $\text{LiHo}_{0.44}\text{Y}_{0.56}\text{F}_4$ (4, 5) suggested that quantum annealing (QA) works better than CA. In QA, temperature is replaced by a quantum mechanical kinetic term; in the specific case, this term is a transverse magnetic field, Γ , mixing the up and down spin states at each site. Initially the quantum perturbation starts out so large in magnitude as to completely disorder the system even at zero temperature. When the transverse field is subsequently re-